Low-temperature magnetotransport in nanometric half-metallic ferromagnetic perovskites



2000 J. Phys.: Condens. Matter 12 3013

(http://iopscience.iop.org/0953-8984/12/13/311)

J. Phys.: Condens. Matter **12** (2000) 3013–3018. Printed in the UK PII: S0953-8984(00)09061-5

# Low-temperature magnetotransport in nanometric half-metallic ferromagnetic perovskites

Ll Balcells, B Martínez, F Sandiumenge and J Fontcuberta†

Institut de Ciència de Materials de Barcelona (CSIC), Campus Universitat Autònoma de Barcelona, E-08193 Bellaterra, Catalunya, Spain

Received 28 October 1999, in final form 7 January 2000

**Abstract.** We have conducted a systematic study of the temperature and magnetic field dependence of the electrical resistivity of granular nanometric $La_{2/3}Sr_{1/3}MnO_3$ ceramics. The results can be analysed within the framework of a model involving the existence of a Coulomb gap, $E_C$, superimposed on a tunnelling barrier between individual grains, which produces a significant blockade at temperatures below ∼100 K. Detailed data analysis allow us to separate the contributions from tunnelling and Coulomb gap and to determine their value and the grain size and magnetic field dependence. It is found that the Coulomb gap increases as $1/\varnothing$ where $\varnothing$ is the mean grain size and the interface surface barrier also becomes more prominent as $\varnothing$ is reduced.

Electrical transport through insulating barriers in granular ferromagnetic materials is receiving a great deal of attention due to the large magnetoresistance observed in some systems. The electron tunnelling probability depends on the relative orientation of the magnetization on neighbouring grains, which can be substantially varied upon application of a magnetic field, thus leading to the so-called tunnel magnetoresistance. In magnetic tunnel junctions the measured magnetoresistance $\mathrm{MR} = (\rho(H) - \rho(0))/\rho(0)$ depends on the spin polarization $P$ of both electrodes (or granules) and the attenuation of the wave-function ($\kappa$) within the barrier of thickness $s$ and height $\varphi$ [1]. It turns out that MR increases with $P$ [2, 3]. Ferromagnetic manganites $L_{1-x}A_xMnO_3$ (L = lanthanide and A = divalent alkaline earth) are especially prone to display large MR due to the fact of their almost complete spin polarization [4]. Indeed, large MR has been observed in $La_{2/3}Sr_{1/3}MnO_3$ ceramics, artificial grain boundaries and tunnel junctions [4–8].

In nanometric grain systems, carriers must overcome the charging energy $E_C = e^2/2C$ of grains of capacitance $C$, thus introducing an additional $\exp(E_C/kT)$ term to the resistivity. As a consequence, at low temperature the resistivity greatly increases giving rise to the so-called Coulomb blockade, which becomes relevant when the size of the metallic particles is reduced. In nanometric metallic ferromagnets both effects should coexist and may lead to novel behaviours. In fact, it has been recently claimed that high-order tunnelling could lead to a significant enhancement of the low-temperature magnetoresistance [9, 10].

The objective of this paper is to study the interplay between spin-polarized tunnelling and Coulomb blockade in nanocrystalline $La_{2/3}Sr_{1/3}MnO_3$ (LSMO). In granular LSMO, insulating barriers can be inherently formed at the grains interfaces [7], where double exchange ferromagnetic interactions are somehow dampened or suppressed [7, 8, 11]. Recently, the existence of a significant contribution of the Coulomb gap to the measured resistivity $\rho(T)$ in $La_{2/3}Sr_{1/3}MnO_3$ ceramics formed by submicrometric grains has been suggested [8]. Indeed, it

† To whom all correspondence should be addressed.

0953-8984/00/133013+06$30.00  

was observed that at low temperature, the resistivity $\rho$ of the samples increases as $\sim \exp(T^{-1/2})$ as predicted by Helman and Abeles [2] for a granular metallic system formed by a broad distribution of grain sizes. From the slope of $\log \rho$ against $T^{1/2}$ an estimate of the Coulomb charging energy $E_C$ was extracted and it was found to be roughly proportional to $1/\varnothing$, where $\varnothing$ is the average size of the granules. We should note however that for a monodisperse granular system the Coulomb barrier is expected to provide an exponential temperature dependence contribution $\sim \exp(T^{-1})$ to the measured resistivity. The predicted (and observed) $\sim \exp(T^{-1/2})$ dependence originates from the assumption that in a granular system there is always a broad distribution of grain sizes [2]. As a consequence, the activation energy extracted from the $\log \rho$–$T^{1/2}$ plots—as done in our previous analysis [8]—does not provide an accurate determination of the charging energy and more refined analysis of the data is required. In this paper we extend further that study including particles as small as 15 nm. Detailed analysis of the resistivity data allows us to separate the contributions from tunnelling and Coulomb gap and to determine their value, and the grain size. In addition, the magnetic field dependence of the Coulomb gap is explored.

$La_{2/3}Sr_{1/3}MnO_3$ ceramics were prepared by a two-step process. First, $La_{2/3}Sr_{1/3}MnO_3$ ceramics were synthesized by conventional high-temperature solid state reaction. The as-grown sample was subsequently ground in an attritor system for 96 h. The x-ray patterns of the as-grown and ground samples are identical except for a notorious broadening of the reflection peaks, due to the reduction of the crystallite size. The mean particle size $\varnothing$, estimated from Sherrer's formula, is about 15 nm, in agreement with transmission electron microscopy (TEM) images which reveal particle sizes comprised between ~6 and ~25 nm. Figure 1 shows HREM images of two nanoparticles having size, ~9 nm (a) and ~25 nm (b). The particle shown in figure 1(a) displays a regular atomic arrangement extending up to the surface of the grain. Figure 1(b) shows a 25 nm nanoparticle displaying lattice fringes. The lattice planes are not disturbed towards the surface as clearly observed in the lower part of the image. Unlike the smaller particle shown in figure 1(a), however, in this case extended defects reaching the surface are observed. The Fourier filtered image shown in the inset reveals that these defects involve a shear displacement perpendicular to the (022) planes. Our observations indicate that the structure of the nanoparticles is typically undisturbed up to the surface, although extended defects may occur within the largest particles.

Pressing of the powders creates samples suitable for transport and magnetic measurements. These were performed using the four-probe method and under magnetic fields up to 55 kOe using a QD SQUID system. Sintering of ceramics at higher temperature allows controlled grain growth [8].

The resistivity temperature $\rho(T)$ of the $\varnothing \approx 15$ nm sample, shown in figure 2 (left/bottom axis), displays a semiconductor-like behaviour at any temperature and a sudden rise of resistivity at temperatures below ≈100 K. This behaviour is a consequence of the nanometric nature of the measured ceramics [8]. See figure 3. In spite of its high resistivity, the sample is ferromagnetic with a Curie temperature $T_C$ of about 360 K as found in single crystals. The magnetization—measured at 1 kOe—against temperature—$M(T)$—reveals that $T_C \approx 360$ K. See figure 2 (right/bottom axis). The shape of the $M(T)$ curve displays typical features of nanostructured ferromagnetic materials [8].

Of the highest significance is the observation that at low temperature (<150 K) $\log \rho$ is proportional to $T^{-1/2}$. This can be clearly appreciated in figure 2 (left/top axis). In figure 3 we show the corresponding $\log \rho$–$T^{-1/2}$ data for samples of various grain sizes. The slope of $\log \rho$ against $T^{-1/2}$ is a measure of the charging energy of the grains ($E_C \sim 1/\varnothing$). Accordingly, it reduces with rising $\varnothing$. As mentioned above, the $\log \rho \sim T^{-1/2}$ temperature dependence is characteristic of transport in granular metallic systems, when the charging energy becomes

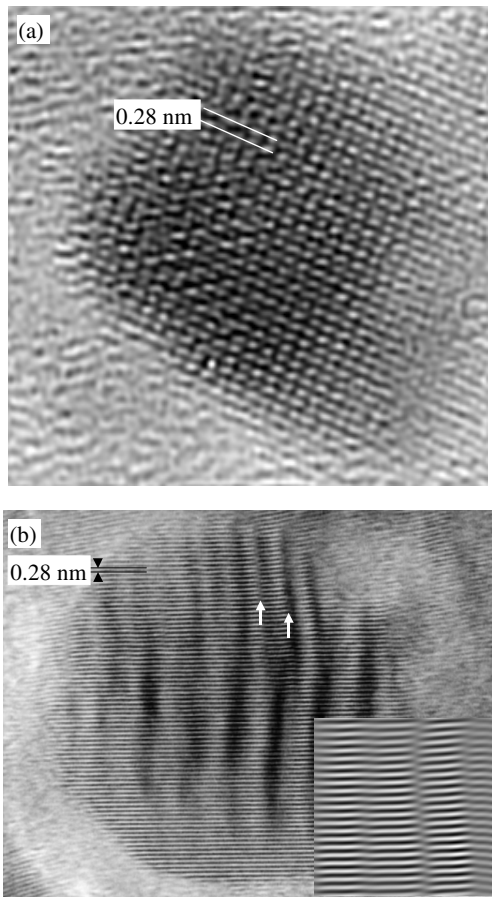


**Figure 1.** (a) High-resolution electron microscopy (HREM) images of a 9 nm LSMO nanoparticle viewed along the [01−1] zone axis. (b) HREM image of a 25 nm nanoparticle displaying (002) lattice fringes. Arrows indicate extended defects. Inset: Fourier filtered image emphasizing the shear displacement across the defects.

important and there is a broad distribution of grain sizes. As discussed in [2], the $T^{-1/2}$ dependence of $\log \rho$ originates from the hypothesis that carrier hopping between granules, a distance $s$ apart, occurs in such a way that $s\kappa E_C$ is a constant. Under these circumstances, it turns out that $\rho(T) \sim \exp 2(\Psi/T)^{1/2}$, where $\Psi \equiv s\kappa E_C$, $\kappa = (2\varphi m_e/\hbar^2)^{1/2}$ and $m_e$ is the electron mass [2]. Consequently, although $\Psi$ should vary with the charging energy, it is not a simple measure of $E_C$. In our preliminary data analysis of [8], this important distinction was not considered.

In figure 4(a) we collect the $\Psi$ values determined for the $\varnothing \approx 15$ nm sample together with data for other grain sizes $\varnothing$. As expected, $\Psi$ increases when reducing the grain size. Data in figure 4(a) can be well described (solid line) by a parabolic-like dependence: $\Psi \sim 1/\varnothing^2$. We emphasize that this dependence reflects the fact that $\Psi$ is not simply proportional to the charging energy ($E_C \sim 1/\varnothing$) of individual grains but also contains the ($s\kappa$) factor, which takes into account the nature (thickness and height) of the tunnel barrier and which can be itself dependent on the grain size. In fact, if $E_C \sim 1/\varnothing$, then in order to account for the observation that $\Psi \sim 1/\varnothing^2$, it turns out that $s\kappa$ should also vary as $\sim 1/\varnothing$.

A rough estimate of $s\kappa$ and its dependence on $\varnothing$ can be obtained from the values of the specific intergranular resistance $R_g \approx \rho^* \varnothing$, measured at a temperature where charging effects are irrelevant, i.e. $kT \gg E_C$. Electric transport across grain boundaries can be viewed as a tunnel process where carriers cross an insulating barrier formed at the grain surface.

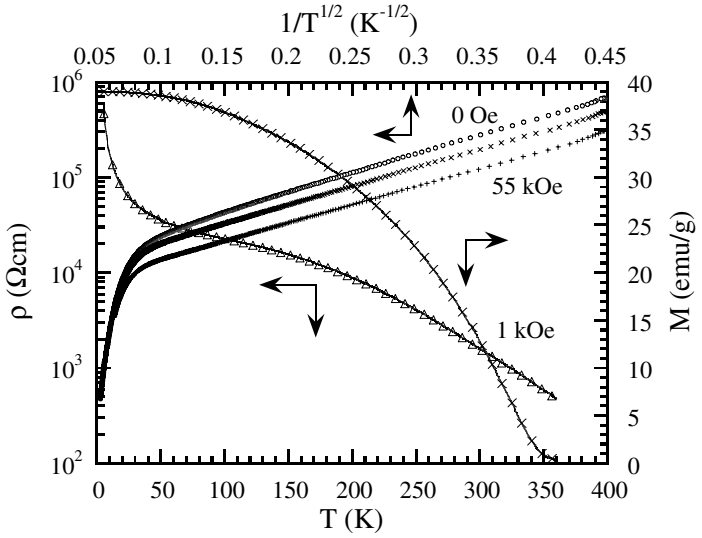


**Figure 2.** The resistivity $\rho(T)$ (left axis) and magnetization $M(T)$ (right axis) (at 1 kOe) against temperature of the $\varnothing \approx 15$ nm sample. Temperature dependence of resistivity ($\log \rho$) of this sample measured at $H = 0$, 10 and 55 kOe against $T^{-1/2}$ (top).

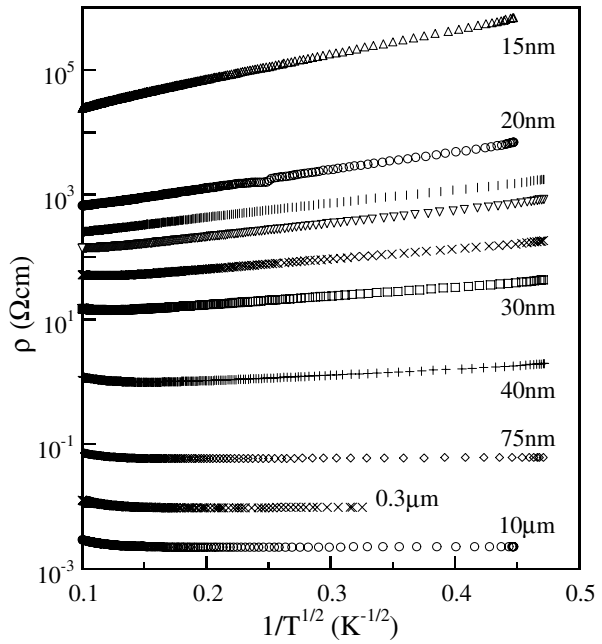


**Figure 3.** Temperature dependence of the resistivity for samples having various grain sizes.

Indications for the existence of an insulating barrier at the grain boundary come from various experiments. For instance: the observation of reduced magnetization of $La_{2/3}Sr_{1/3}MnO_3$ particles of reduced size has been interpreted as due to the existence of a non-collinear surface layer [8]. Frustrated magnetic interaction in double exchange manganites should be

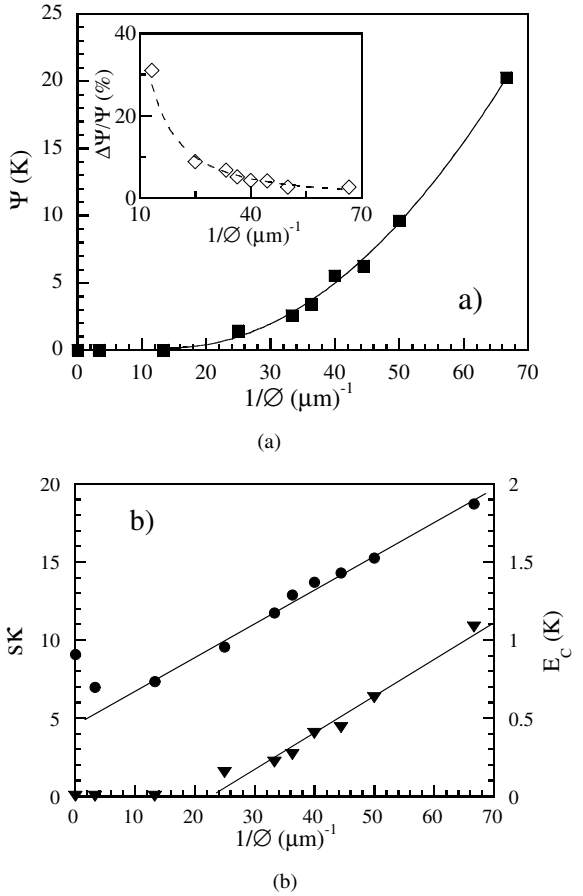


**Figure 4.** (a) Grain size dependence of the slopes $\Psi$ of $\rho(T^{-1/2})$. The solid line through the data is a fit to the law $\Psi \sim 1/\varnothing^2$. Inset: relative variation of the slope $\Delta\Psi$ ($H = 10$ kOe)/$\Psi(0)$ as a function of $\varnothing$. (b) Grain size dependence of $s\kappa$ (circles, left) and $E_C$ (triangles, right).

accompanied by carrier localization at interfaces. Artificial insulating barriers have also been created in $La_{2/3}Sr_{1/3}MnO_3/SrTiO_3/La_{2/3}Sr_{1/3}MnO_3$ heterostructures where the conductance has been clearly described in terms of a tunnel mechanism [4]. According to tunnelling models, in the ohmic regime, the resistance across a barrier is given by $R_g \approx R_0(s/\kappa)\exp(2s\kappa)$ where $R_0$ contains only universal constants [12] and $s$ and $\kappa$ have been defined above. Consequently, using this expression and the measured $R_g$ data, the $s\kappa$ values can be estimated. In figure 4(b) we plot $s\kappa$ against $1/\varnothing$, with $R_g$ evaluated from the $\rho(100\ \mathrm{K})$ data of figure 3. This plot reveals that $s\kappa$ increases when reducing the grain size, thus meaning that interface barriers become more relevant when reducing $\varnothing$. This observation is in agreement with recent suggestions of an increasingly thicker non-metallic layer at the interfaces as the grain size [8] or the thickness of LSMO thin film are reduced [13].

It is illustrative to evaluate the charging energy $E_C = \Psi/s\kappa$ from the experimentally measured slopes $\Psi$ and the $s\kappa$ values from figures 4(a) and 4(b). In figure 4(b) (right) we show the obtained $E_C$ values. It is clear that $E_C \sim 1/\varnothing$ as expected. Data in figure 4(b) provide strong evidence for the contribution of the Coulomb blockade to the zero-field resistivity of nanometric LSMO ceramics, which is superimposed on the spin dependent

tunnelling contribution. However, it is important to notice that the charging energy values are significantly lower than those that would be extracted from the simplest approximation $\rho(T) \sim \exp(E_C/kT)^{1/2}$ used in [8]. Although small $E_C$ values have also been reported for some other half-metallic granular ferromagnets such as $CrO_2$ [14] this is not genuine for this class of ferromagnetic metallic oxides; indeed in Co–Al–O granular films [9], a Coulomb gap of about $E_C \approx 9$ K has been found, contributing to the overall resistivity up to 300 K.

On the other hand, it has been suggested that cotunnelling processes in the Coulomb blockade regime may lead to large MR [10]. Therefore in the following we will search for any additional contribution to MR arising from the Coulomb blockade. To that purpose we have performed measurements of $\rho(T)$ under magnetic field and we have extracted the slopes $\Psi$. The $\rho$–$T^{-1/2}$ data for the $\varnothing \approx 15$ nm sample under various fields are included in figure 2. This figure indicates a gradual lowering of the slope $\Psi$ when increasing the magnetic field. However measurements of $\Psi(H)$ for samples having different grain sizes reveals that the relative change $\Delta\Psi(H)/\Psi(0) = (\Psi(H) - \Psi(0))/\Psi(0)$, particularly in the low-field region, progressively reduces when reducing $\varnothing$. See the inset in figure 4(a). This means that in the limit of nanometric particles, where the Coulomb gap is expected to be dominant, there is a vanishingly small variation of the slope with field: i.e. the Coulomb blockade regime does not show any MR.

In summary, we have provided evidence that in nanocrystalline LSMO, the Coulomb blockade coexists with spin dependent tunnelling between grains, thus leading to a significant enhancement of resistivity at low temperature. The fact that the Coulomb barrier is found to be independent of the magnetic field suggests that high-order tunnelling processes are not relevant and conduction is dominated by charge transfer between grains of similar size.

## Acknowledgments

We thank Professor F Guinea for useful discussions. Financial support by the CICYT (MAT97-0699 and MAT99-0984) and the CEE-OXSEN projects and the Generalitat de Catalunya (GRQ99-00363) are acknowledged.

## References

[1] Landauer R 1997 *Phil. Mag.* **21** 863
[2] Helman J S and Abeles B 1976 *Phys. Rev. Lett.* **37** 1429
[3] Inoue J and Maekawa S 1996 *Phys. Rev.* B **53** R11 927
[4] Viret M, Drouet M, Nassar J, Contour J P, Fermon C and Fert A 1997 *Europhys. Lett.* **39** 545
[5] Hwang H Y, Cheong S-W, Ong N P and Batlogg B 1996 *Phys. Rev. Lett.* **77** 2041
Mahesh R, Mahendiran R, Raychaudhuri A K and Rao C N 1996 *Appl. Phys. Lett.* **68** 2291
Sánchez R D *et al* 1996 *Appl. Phys. Lett.* **68** 1
Li X W, Gupta A, Xiao Gang and Gong G Q 1997 *Appl. Phys. Lett.* **71** 1124
Gupta A *et al* 1996 *Phys. Rev.* B **54** R15 629
[6] Mathur N D *et al* 1997 *Nature* **387** 266
[7] Fontcuberta J, Martínez B, Laukhin V, Balcells Ll, Obradors X, Cohenca C H and Jardim R 1998 *Phil. Trans. R. Soc.* A **356** 1577
[8] Balcells Ll, Fontcuberta J, Martínez B and Obradors X 1998 *Phys. Rev.* B **58** R14 697
[9] Mitani S, Takahashi S, Takanashi K, Yakushiji K, Maekawa S and Fujimori H 1998 *Phys. Rev. Lett.* **81** 2799
[10] Takahashi S and Maekawa S 1998 *Phys. Rev. Lett.* **80** 1758
[11] Park J-H *et al* 1998 *Phys. Rev. Lett.* **81** 1953
[12] Simmons J G 1963 *J. Appl. Phys.* **34** 1793
[13] Sun J Z, Abraham D W, Rao R A and Eom C B *Preprint* Cond-mat/9809414
[14] Coey J M D, Berkowitz A E, Balcells Ll, Putris F F and Barry A 1998 *Phys. Rev. Lett.* **80** 3815